

Weakly Interacting Bose Mixtures at Finite Temperature

Bert Van Schaeybroeck

*Instituut voor Theoretische Fysica,
Katholieke Universiteit Leuven,*

Celestijnenlaan 200 D, B-3001 Leuven, Belgium.

(Dated: November 20, 2018)

Motivated by the recent experiments on Bose-Einstein mixtures with tunable interactions we study repulsive weakly interacting Bose mixtures at finite temperature. We obtain phase diagrams using Hartree-Fock theory which are directly applicable to experimentally trapped systems. Almost all features of the diagrams can be characterized using simple physical insights. Our work reveals two surprising effects which are dissimilar to a system at zero temperature. First of all, no pure phases exist, that is, at each point in the trap, particles of both species are always present. Second, even for very weak interspecies repulsion when full mixing is expected, *condensate* particles of both species may be present in a trap without them being mixed.

PACS numbers: 03.75.Hh, 03.75.Mn, 67.60.Bc, 67.85.Fg

Introduction – Since the early realization of mixtures of Bose-Einstein condensates (BECs) ten years ago [1], a host of experiments revealed the rich physics of two-component Bose [2, 3] and Fermi [4] systems. Whereas most experiments use mixtures of hyperfine states of like atomic species, it is also possible for unlike species to be trapped simultaneously. Moreover both systems allow the use of Feshbach resonances by means of which the interatomic interactions can be tuned to arbitrary values and which revolutionized the physics of ultracold gases. Such resonances were observed for binary Bose gases consisting of ^{87}Rb – ^{41}K [5], ^{87}Rb – ^{133}Cs [6] and ^{85}Rb – ^{87}Rb [7, 8] mixtures; clear phase segregation was achieved for the last mixture by changing the intraspecies interactions of the ^{85}Rb particles [8].

To date theoretical works on BEC mixtures predominantly focussed on static and dynamic properties at zero temperature [9]. Interesting questions, however, can be posed concerning the finite temperature regime: for instance, will, upon increasing the interspecies repulsion, phase segregation for thermally depleted particles set in at the same time as for condensate particles? Does increasing the temperature induce an increased tendency to mix the species? Can pure phases still exist? The issue of phase segregation at nonzero temperature was already addressed in Ref. 10 where the authors calculated the conditions for an instability to occur in a volume with fixed particle numbers. Also the case of a Bose mixtures in a trap at nonzero temperature was briefly discussed.

In this Letter, we aim at clarifying the possible phase structures in traps of Bose mixtures at finite temperature. The presented phase diagrams are directly applicable to

trapped situations, and yet, independent of the specific trapping parameters. We realize this by drawing the diagrams as a function of the chemical potentials of the two species while taking the temperature to be fixed. These diagrams are apt for gases confined by a smoothly varying potential for then the use of a local density approximation is appropriate and an effective chemical potential can be taken as locally constant at each position in the trap. Rather than giving exact diagrams using specific parameters [17], we focus here on their basic understanding by highlighting the generic features; more elaborate work will be presented in a forthcoming paper. We argue that our diagrams can be almost fully characterized, based on the knowledge of single-species Bose systems at finite temperature and the BEC mixture at zero temperature.

Equation of state — Consider two Bose species, labelled 1 and 2, at temperature T and at chemical potentials μ_1 and μ_2 . The particles of species i and j interact weakly via s-wave scattering, quantified by a positive scattering length a_{ij} and a coupling constant $G_{ij} = 2\pi\hbar^2 a_{ij} (m_i^{-1} + m_j^{-1})$ (henceforth $i, j = 1, 2$). We use the self-consistent Hartree-Fock (HF) equations of state as first introduced by Huang et al. [11]. This very model is known to give good agreement with experiments [12] and even with quantum Monte Carlo simulations [13]. The HF model treats noncondensed particles as free particles with a mean field chemical potential shift, and takes only thermal and no quantum fluctuations into account. The HF grand potential per unit volume Ω is expressed in terms of the condensate densities n_{ci} and thermally depleted densities n_{di} [3, 11]:

$$\Omega = \sum_{i=1,2} \left[-\frac{g_{5/2}(e^{\beta\mu_i^0}) k_B T}{\lambda_i^3} + \mu_i^0 n_{di} + G_{ii} \left(\frac{n_{ci}^2}{2} + 2n_{ci} n_{di} + n_{di}^2 \right) - \mu_i (n_{ci} + n_{di}) \right] + G_{12} (n_{c1} + n_{d1})(n_{c2} + n_{d2}),$$

where $\lambda_i = \sqrt{2\pi\hbar^2/(m_i k_B T)}$, $\beta = 1/k_B T$ and $g_l(x) = \sum_{s=1}^{\infty} s^{-l} x^s$. The first two terms are due to the entropy and the kinetic energy of the depleted particles. The very last term couples the two species by repulsive interactions. At fixed chemical potential, minimization of Ω with respect to the densities n_{c_i} and n_{d_i} yields the self-consistent Hartree-Fock equations of state:

$$\mu_1 = \mu_1^0 + 2G_{11}(n_{c_1} + n_{d_1}) + G_{12}(n_{c_2} + n_{d_2}), \quad (1a)$$

$$\mu_2 = \mu_2^0 + 2G_{22}(n_{c_2} + n_{d_2}) + G_{12}(n_{c_1} + n_{d_1}), \quad (1b)$$

and, $\mu_i^0 = -G_{ii}n_{c_i}$ whenever $n_{c_i} \neq 0$. The depleted densities on the other hand are governed by minimization with respect to μ_i^0 :

$$n_{d_i} = g_{3/2}(e^{\beta\mu_i^0})/\lambda_i^3. \quad (2)$$

For most systems of ultracold gases only few length-scales are relevant. These include the particle de Broglie wavelength λ_i , the interparticle distance $n_i^{-1/3}$ and lastly the scattering lengths a_{ij} . The HF theory as introduced above is valid in case of weak interactions i.e. for small values of a_{ij}/λ_i and when *single*-particle excitations prevail i.e. when $n_i a_{ij} \lambda_i^2 \ll 1$ [2]. Also, the theory fails very close to the transition point where fluctuations become dominant. In nowadays experiments, the scattering length takes values of order of ten nanometers and below, whereas the interparticle distances and the Broglie wavelengths are typically of the order of microns and higher. It follows that the necessary conditions for the HF theory to be valid are fulfilled [18].

We proceed by first discussing BEC mixtures at zero temperature and a single species Bose gas at finite temperature, since these systems provide all ingredients necessary for the understanding of the results obtained further.

BEC mixture at $T = 0$ — At zero temperature, the HF theory reduces to Gross-Pitaevskii (GP) theory for a spatially homogeneous system. According to GP theory, two regimes can be distinguished, depending on the parameter Δ defined as [9]:

$$\Delta = G_{11}G_{22}/G_{12}^2 - 1. \quad (3)$$

When $\Delta < 0$, the inter-species repulsion is sufficiently strong to induces phase segregation and solely BEC 1 or BEC 2 may exist as ground states, that is, species 1 and 2 are immiscible. One readily finds the following conditions:

$$\text{BEC 1 when } \mu_1 > \mu_2 \sqrt{G_{11}/G_{22}}, \quad (4a)$$

$$\text{BEC 2 when } \mu_1 < \mu_2 \sqrt{G_{11}/G_{22}}. \quad (4b)$$

On the other hand, when $\Delta > 0$, the interspecies repulsion is weak and a mixed phase of nonzero density of BEC 1 and BEC 2, here denoted as BEC MIX, may appear as the ground state:

$$\text{BEC MIX when } G_{12}/G_{22} < \mu_1/\mu_2 < G_{11}/G_{12}. \quad (5)$$

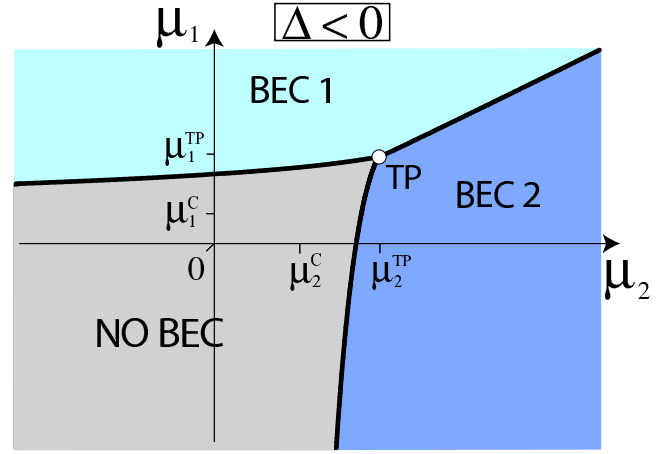


FIG. 1: (Color online) Generic phase diagram for two Bose species at fixed temperature in case of strong interspecies repulsion ($\Delta < 0$) as a function of the chemical potentials of both species. The BEC 1 (green) phase consists of condensate particles of species 1 and thermally depleted particles of species 1 and 2 and vice versa for the BEC 2 (blue) phase. The (grey) phase NO BEC consists of depleted particles of both species. The chemical potential μ_i^C is given by Eq. (6) and the locus of the triple point TP is given in Eq. (7) while the first-order phase boundaries are described by Eqs. (8), (9) and (10).

Single-species at finite T — Consider now a gas of species i at fixed temperature. One can think of the chemical potential μ_i as a measure for the particle density: the higher μ_i , the higher the density of species i . For large and negative values of μ_i , the system is dilute and the interaction energy small. On the other hand, above a certain “critical” positive chemical potential a transition to a phase with nonzero condensate density sets in; by the HF approach, this critical value is attained when $\mu_i^0 = 0$ such that [3] [19]:

$$\mu_i^C = 2G_{ii} \zeta(3/2)/\lambda_i^3, \quad (6)$$

with ζ the Riemann zeta function. Note that μ_i^C depends on temperature via λ_i and from the scaling $\mu_i^C \simeq k_B T (a_{ii}/\lambda_i)$ we conclude that $\mu_i^C \ll k_B T$.

The introduction of a second Bose gas will shift the critical chemical potential to a higher value than μ_i^C ; this can be ascribed to the interspecies repulsion which tends to rarify the gas of species i .

Phase Diagram for $\Delta < 0$ and finite T — Upon working at fixed particle numbers as in Ref. 10, the onset of phase segregation can be naturally probed by the presence of a density instability. At fixed chemical potentials on the other hand, this method is inadequate as an instability indicates a spinodal (line) rather than the transition itself in case it is of first order. Instead, we have compared numerically the grand potentials for the eight possible thermodynamical phases and their associated multiple solutions. We arrive at the generic phase diagrams for Bose mixtures at finite temperature in Figs. 1 and 2 for the cases $\Delta < 0$ and $\Delta > 0$ respectively.

Identical to the behavior at $T = 0$, no mixing of unlike condensate particles is possible at finite T when $\Delta < 0$. Only three phases appear in Fig. 1, none of which are pure; that is, even for extremely strong interspecies repulsion, depleted particles of both species are present in all phases. Accordingly, BEC 1 denotes the phase composed of condensate particles of species 1 and depleted particles of both species, and vice versa for BEC 2. The NO BEC phase denotes the phase with thermal particles of species 1 and 2.

A triple point TP is present in the phase diagram of Fig. 1. As checked numerically, its locus (μ_1^{TP}, μ_2^{TP}) can be found by setting $\mu_1^0 = \mu_2^0 = 0$ in Eq. (1):

$$\mu_1^{TP} = \mu_1^C + \mu_2^C G_{12} / 2G_{22}, \quad (7a)$$

$$\mu_2^{TP} = \mu_2^C + \mu_1^C G_{12} / 2G_{11}. \quad (7b)$$

Note that in units of μ_1^C and μ_2^C , the position of point TP is temperature independent.

Consider now the phase boundary between BEC 1 and 2; for large and positive values of both chemical potentials, the interaction energy per particle will eventually become much larger than the thermal energy and so asymptotically the $T = 0$ behavior is expected. Indeed, we find that in accord with Eq. (4) the BEC 1-2 phase boundary satisfies:

$$\mu_1 / \mu_2 = \sqrt{G_{11} / G_{22}} \text{ when both } \mu_1, \mu_2 \rightarrow \infty. \quad (8)$$

Moving along the NO BEC-BEC 1 boundary away from TP, the density of species 2 decreases; in the limit of $\mu_2 \rightarrow -\infty$, only particles of species 1 remain such that the single-component value $\mu_1 \rightarrow \mu_1^C$ is attained. The associated asymptotic decay is exponential as the NO BEC-BEC 1 phase boundary is described by:

$$\mu_1 = \mu_1^C + G_{12} e^{\mu_2 / k_B T} / \lambda_2^3 \text{ when } \mu_2 \rightarrow -\infty. \quad (9)$$

Because $\mu_2^C \ll k_B T$, it follows that the asymptotic convergence is slow if μ_2 is expressed in units of μ_2^C . The same line of argument with interchanged indices 1 and 2 applies to the demarcation line between BEC 2 and NO BEC:

$$\mu_2 = \mu_2^C + G_{12} e^{\mu_1 / k_B T} / \lambda_1^3 \text{ when } \mu_1 \rightarrow -\infty. \quad (10)$$

In outline, we have shown that one can qualitatively establish the phase diagram for the case $\Delta < 0$ without explicitly performing any numerics. Indeed, we found that the expressions for the triple point (Eq. (7)), and the phase boundaries (Eqs. (8)-(10)) agree well with the numerically exact results.

Phase Diagram for $\Delta > 0$ at finite T — At zero temperature mixing of unlike condensate particles is possible when Δ is positive. We find the same behavior at finite T . This is shown in Fig. 2 where BEC MIX consists of condensed and depleted particles of both species. The bifurcation of the BEC 1-2 line brings along the appearance of a new triple point TP2 (TP1 is identical to TP of Fig. 1). For the aforementioned reasons, the $T = 0$ physics is recovered for large and positive chemical potentials. Hence

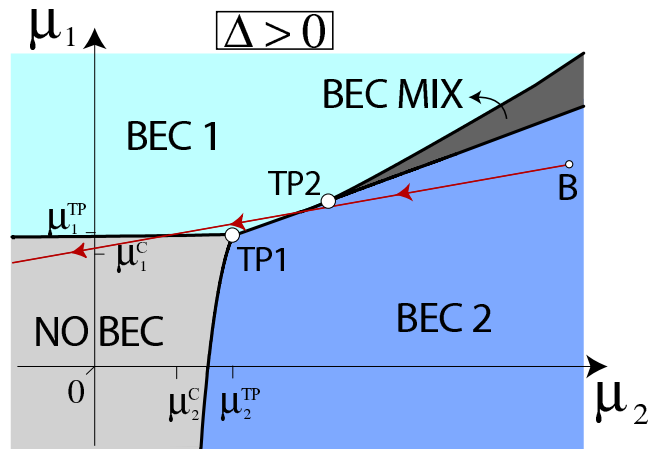


FIG. 2: (Color online) The same applies as in Fig. 1 except that weak interspecies interactions are considered ($\Delta > 0$). The (dark grey) BEC MIX phase consists of condensed and depleted particles of both species. The red arrowed line indicates a possible tracing of the diagram as a function of the (radial) position in the trap. The point B indicates the chemical potentials at the center of the trap.

Eq. (5) implies that the BEC MIX phase is delimited by the phase boundaries

$$\begin{cases} \mu_1 / \mu_2 = G_{11} / G_{12} \\ \mu_1 / \mu_2 = G_{12} / G_{22} \end{cases} \text{ when both } \mu_1, \mu_2 \rightarrow \infty. \quad (11)$$

The location of triple point TP2 alters upon varying temperature and Δ . For small and positive values of Δ , TP2 enters at large and positive values of the chemical potentials while TP2 coalesces with TP1 only in the limit $\Delta \rightarrow \infty$. This leads us to a remarkable conclusion: even when the zero temperature condition for species mixing is satisfied, at finite temperature, two-phase equilibrium between BEC 1 and 2 is still allowed. Changing the temperature also induces a displacement of TP2 with respect to TP1. Intuitively one expects that increasing the temperature favors mixing. Yet, condensate particles carry no entropy and we find rather the opposite: increasing the temperature suppresses mixing. In particular, the distance between TP1 and TP2 (in units of μ_i^C) increases upon increasing the temperature.

In the ideal case of fully suppressed interspecies interactions ($\Delta \rightarrow \infty$) the triple points TP1 and TP2 coincide and, as expected, the phase boundaries are the horizontal and vertical lines $\mu_1 = \mu_1^C$ and $\mu_2 = \mu_2^C$.

To summarize, the $\Delta > 0$ phase diagram is similar to the $\Delta < 0$ diagrams but is marked by the appearance of an additional phase consisting of mixed BEC species, and an additional triple point TP2. Despite the known asymptotic behavior of the phase boundaries around the BEC MIX phase (see Eq. (10)), the locus of TP2 depends in a non-trivial way on temperature and Δ and must therefore be determined numerically.

Discussion — In order to extract from Figs. 1 and 2 the possible phase structures appearing in an experimental trap, the trapping potentials U_i are required. In most experiments a local density approximation or Thomas-Fermi approximation is justified such that at each position \mathbf{r} an effective chemical potential $\mu_i(\mathbf{r}) = \mu_i - U_i(\mathbf{r})$ may be assumed constant; $\mu_i(\mathbf{r})$ is maximal at the center and minimal at the edge of a trap. In case both species are harmonically confined or $U_i(\mathbf{r}) = m_i \omega_i^2 \mathbf{r}^2 / 2$, the chemical potentials probe our phase diagrams following a straight line:

$$m_2 \omega_2^2 (\mu_1(\mathbf{r}) - \mu_1) = m_1 \omega_1^2 (\mu_2(\mathbf{r}) - \mu_2). \quad (12)$$

As an example, a trap configuration which is described by the red path in Fig. 2 contains a BEC 2 core surrounded by shells of BEC 1 and NO BEC. Note that our phase diagrams do not explicitly depend on trapping parameters nor gravity.

The most striking conclusion of this work is that no pure phases exist at finite temperature; even for large interspecies interactions, the depleted particles are not entirely expelled [20]. However, the fact that upon increasing the interspecies repulsion G_{12} in the BEC MIX phase, condensate particles will be expelled first, may be understood from the following simplistic argument: in the expression for Ω , it is seen that due to different exchange terms the intraspecies interactions for depleted particles are a factor 2 higher than those of condensate particles. A naive application of the zero-temperature criterion for phase segregation ($G_{12} > \sqrt{G_{11} G_{22}}$) to depleted particles, yields segregation for values of G_{12} higher than $\sqrt{2G_{11} G_{22}}$.

As a direct extension of this work, the interface physics and its impact on the phase structures can be explored in case of two-phase equilibrium. A generalization of our HF theory to spatially inhomogeneous systems is thereby required; within a first approximation, this can be effectuated by introducing the terms $\nabla^2 \sqrt{n_{ci}}$ into the grand potential [3]. Such theory would then allow the calculation of surface excess quantities which are useful for tightly confined gases where their effect on the ground state configuration turns out to be substantial [8, 14, 15]. Further challenges include a generalization of the theory of anomalous wetting phase transitions to finite temperatures [16].

Conclusion — We have elaborated generic phase diagrams for Bose mixtures at finite temperature based on the Hartree-Fock model. As corroborated by numerical analysis, almost all properties of our phase diagrams can be expressed in terms of known results for single-species gases at finite temperature and for binary mixtures at zero temperature. This means that it is possible to establish the phase diagrams (aside from the triple point TP2 in case $\Delta > 0$) without performing any numerics. The phase diagrams are drawn as a function of the chemical potentials of

the species such that, spatially tracing the trap is equivalent to exploring the phase diagram. We highlight the importance of the triple points in our diagrams and find that, surprisingly, no pure phases exist, and, increasing the temperature tends to suppress the mixing of condensate particles.

Acknowledgement — The author thanks Lev Pitaevskii, Joseph Indekeu and Achilleas Lazarides for useful suggestions. B.V.S. is a Postdoctoral Fellow of FWO.

-
- [1] J. Stenger et al., Nature (London) **396**, 345 (1998); D.S. Hall et al., Phys. Rev. Lett. **81**, 1539 (1998).
 - [2] C.J. Pethick and H. Smith, *Bose-Einstein Condensation in Dilute Gases* (Cambridge Press, Cambridge, 2002).
 - [3] L.P. Pitaevskii and S. Stringari, *Bose-Einstein Condensation* (Clarendon Press, Oxford, 2003).
 - [4] S. Giorgini et al., Rev. Mod. Phys. **80**, 1215 (2008).
 - [5] G. Thalhammer et al., Phys. Rev. Lett. **100**, 210402 (2008).
 - [6] K. Pilch et al., arXiv:0812.3287v1.
 - [7] S.B. Papp et al., Phys. Rev. Lett. **97**, 180404 (2006).
 - [8] S.B. Papp et al., Phys. Rev. Lett. **101**, 040402 (2008).
 - [9] P. Ao and S.T. Chui, Phys. Rev. A **58**, 4836 (1998); P. Öhberg and S. Stenholm, *ibid.* **57**, 1272 (1998); F. Riboli and M. Modugno, *ibid.* **65**, 063614 (2002); D.M. Jezek and P. Capuzzi, *ibid.* **66**, 015602 (2002); S. Ronen et al., *ibid.* **78**, 053613 (2008); T.-L. Ho and V.B. Shenoy, Phys. Rev. Lett. **77**, 3276 (1996); C.K. Law et al., *ibid.* **79**, 3105 (1997); B.D. Esry et al., *ibid.* **78**, 3594 (1997); E. Timmermans, *ibid.* **81**, 5718 (1998); S.G. Bhongale et al., *ibid.* **100**, 185301 (2008); M. Trippenbach et al., J. Phys. B **33**, 4017 (2000).
 - [10] H. Shi et al., Phys. Rev. A **61**, 063613 (2000).
 - [11] K. Huang et al., Phys. Rev. **105**, 776 (1957); K. Huang, *Statistical Mechanics*, 2nd Ed. (Wiley, NY, 1987); N.P. Proukakis and B. Jackson, J. Phys. B **41**, 203002 (2008).
 - [12] F. Gerbier et al., Phys. Rev. A **70**, 013607 (2004).
 - [13] M. Holzmann et al., Phys. Rev. A **59**, 2956 (1999).
 - [14] B. Van Schaeybroeck, Phys. Rev. A. **78**, 023624 (2008).
 - [15] G.B. Partridge et al., Phys. Rev. Lett. **97**, 190407 (2006).
 - [16] J.O. Indekeu et al., Phys. Rev. Lett. **93**, 210402 (2004).
 - [17] Our diagrams differ for different values of (the later introduced) six parameters: $m_1, m_2, a_{11}, a_{22}, a_{12}$ and T . Since even the scattering lengths vary in experiments, we limit our discussion to generic features.
 - [18] The scattering length is known to diverge near a Feshbach resonance. Nevertheless, our theory still applies to the experiments of Ref. 8 since the largest values of $n_i a_{ij} \lambda_i^2$ are around 0.1.
 - [19] Small corrections apply near the critical points, due to the first-order nature of the transition; as mentioned before, the theory is not accurate very close to the transition point.
 - [20] This very effect therefore vanishes at zero temperature when the depleted densities are quenched.